UC Irvine
UC Irvine Previously Published Works

Title

Anisotropy of the normal state properties of the superconducting Co1−xNixZr2 system

Permalink

Journal

ISSN

Authors

Henkie, Z
Fertig, WA
Fisk, Z
et al.

Publication Date

DOI

Copyright Information

Peer reviewed

Anisotropy of the Normal State Properties of the Superconducting $Co_{1-x}Ni_xZr_2$ System*

Z. Henkie,† W. A. Fertig,‡ Z. Fisk,§ D. C. Johnston,‖ and M. B. Maple

Institute for Pure and Applied Physical Sciences, University of California—San Diego, La Jolla, California

Anisotropic behavior of the normal state thermoelectric power, electrical resistivity, and magnetic susceptibility is reported for the superconducting $Co_{1-x}Ni_xZr_2$ system.

1. INTRODUCTION

There is currently much experimental and theoretical activity dealing with the influence of crystalline anisotropy on superconductivity. Of particular interest are compounds which crystallize in the tetragonal $CuAl_2$ structure (C-16). The Al atoms form planar nets between which are sandwiched the Cu atoms; the latter form linear chains running parallel to the unique crystallographic c axis. Havinga *et al.*[1] examined 46 systems with the $CuAl_2$ crystal structure and found that 25 of them become superconducting above 0.07 K.

Fragmentary experimental evidence in the literature suggests that the superconducting and normal state properties of some members of this group of compounds may be anisotropic. Tagano *et al.*[2] and Tagano and Tachikawa[3] reported anisotropy of the critical current density and upper critical field H_{c2} of a $RhZr_2$ sample possessing a simple fiber texture obtained by slow cooling from the arc-melted state. They extrapolated their data for H_{c2} to zero temperature and found a rather high value of

†Permanent address: Institute for Low Temperature and Structure Research, Polish Academy of Sciences, Wroclaw, Poland.
‡Deceased.
§Present address: Los Alamos National Laboratory, Los Alamos, New Mexico.
‖Present address: Corporate Research Laboratories, Exxon Research and Engineering Co., Linden, New Jersey.

106.5 kG. Eshelman and Smith[4] found anisotropic ultrasonic wave velocities in a single crystal of $NiZr_2$, which they grew in a tungsten crucible using the Bridgman technique. The temperature dependence of the elastic constants, particularly C_{66}, was atypical and indicated a significant degree of mode softening at low temperatures, a behavior similar to that exhibited by Nb_3Sn and V_3Si. Some samples of $(Fe, Co)Zr_2$ and $NiZr_2$–$CoTa_2$ solid solutions showed preferred orientation of the crystallites and anisotropy of the thermoelectric power.[1]

Havinga and van Maaren[5] found that the superconducting transition temperature T_c, room-temperature magnetic susceptibility, and thermoelectric power of C-16 systems were oscillatory functions of n, the valence electron concentration per atom, with a larger number of oscillations than might be anticipated on the basis of Matthias' rules.[5,6] The first pronounced maximum in T_c vs. n occurred at $n^{max} \lesssim 2.4$. The number of valence electrons was determined in the following manner: if the minor constituent was a transition metal, then its d band was assumed to be full and the remainder of the valence electrons of the constituents was taken as the total number of valence electrons of the substance.

In the $Co_{1-x}Ni_xZr_2$ system, n increases through the value of n^{max}, from 2.33 to 2.67, as x increases from 0 to 1. Yamaha et al.[7] reported a maximum $T_c = 5.9$ K for $x = 0.15$. Subsequent studies by McCarthy[8] and Havinga et al.[1] have confirmed a maximum in T_c at a similar concentration. Such interesting superconducting behavior in the $Co_{1-x}Ni_xZr_2$ system has prompted the present investigation of the normal state properties of this system. Presented here are measurements of the thermoelectric power, magnetic susceptibility and electrical resistivity, and of the anisotropy in these properties for single-crystal samples with $0 \leqslant x \leqslant 0.29$.

2. EXPERIMENTAL PROCEDURE

The Bridgman method was employed to grow $Co_{1-x}Ni_xZr_2$ crystals with $x = 0.0$, 0.154, 0.21, and 0.290. Stoichiometric amounts of etched Zr (Materials Research Corp., 99.99% pure), Co (Johnson-Matthey, 99.99% pure), and Ni (Johnson-Matthey, 99.99% pure) were arc-melted on a water-cooled copper hearth under an argon atmosphere. Ingot inversion between each of the several meltings facilitated sample homogenization. Each sample was then placed inside a conical-tipped graphite crucible which had been previously outgassed in vacuo at 1200°C. Next, the sample and crucible were outgassed together in vacuo at 900°C inside a quartz tube, which was subsequently sealed when the pressure had been reduced to below 10^{-5} Torr. Crystals were grown by lowering the sealed tubes at the rate of 1.5 cm/h, first through a zone with a homogeneous temperature

of 1200°C and then through a zone with a vertical temperature gradient of 80°C/cm.

A small sand-blasting machine was used to gently remove the graphite from the samples, which were subsequently cleaned by etching in a solution of HF, HNO_3, and H_2O in the proportions $1:1:20$. The crystallographic orientations of the samples were determined by the x-ray backreflection Laue technique. Fracturing of the crystals presented some difficulties. When the z axis of the growing crystals deviated from the longitudinal axis of the crucible, surface cracks, mostly parallel to (110) planes, were observed in the solidified sample. Nevertheless, examination by the standard Laue method revealed no detectable differences in crystallographic orientation for crystals 15–25 mm long and up to 8 mm in diameter. After the orientation procedure, the crystals were spark-cut to their final dimensions. For the thermopower and resistivity measurements, rectangular parallelopipeds 0.4 mm wide, 0.4 mm thick, and 7–15 mm long were cut in the $\langle 100\rangle$, $\langle 110\rangle$, $\langle 112\rangle$, $\langle 111\rangle$, $\langle 101\rangle$, and $\langle 001\rangle$ directions. The samples for magnetic susceptibility measurements were of irregular shape and of mass ~ 0.3 g.

The thermoelectric power of a sample was measured by placing the crystal between two copper blocks. A gallium–indium eutectic liquid of composition $Ga_{83.5}In_{16.5}$ was used to improve both the electrical and thermal contact between sample and copper blocks. Each block was surrounded by a copper thermal shield, which had a hole for the sample to pass through and Teflon to provide electrical isolation between the block and the thermal shield. An electrical heater attached to one of the shields maintained a temperature difference of 20–25 K between sample ends during the actual measurements. Due to the presence of the copper shields, the temperature gradient was minimized near the block–sample interfaces, so that these junctions could be considered to be isothermal. Copper wires attached to the two-block–sample interfaces carried the thermoelectric voltage signal to a digital voltmeter. This instrument could also monitor the signals from a copper–constantan thermocouple anchored to each copper block and also from one held at a reference temperature of 0°C. In this way both the temperature of the colder copper block and the differential temperature across the sample could be determined.

The accuracy and resolution of the voltmeter permitted thermoelectric powers of samples with respect to copper to be established within $\pm 0.05\ \mu V/K$. Before actual measurements on the $Co_{1-x}Ni_xZr_2$ system were made, the entire experimental assembly was tested by measuring the thermoelectric power of both 99.99% pure silver and platinum. The data were reproducible within the limits of accuracy, but the measured values differed from those calculated by using the absolute thermoelectric power results for copper, silver, and platinum given by Cusack and Kendall.[9] The

maximum discrepancy between the calculated and measured values occurred at 273 K and was equal to $+0.09 \, \mu V/K$ for silver and $-0.46 \, \mu V/K$ for platinum. These numbers set upper limits to the inaccuracies of the $Co_{1-x}Ni_xZr_2$ thermoelectric power data presented here if the data of Cusack and Kendall for the absolute thermoelectric power of copper are accepted.

3. RESULTS

The results of the absolute thermoelectric power for the $Co_{1-x}Ni_xZr_2$ system over the temperature range 100–400 K are presented in Fig. 1 for $x = 0.0$, in Fig. 2a for $x = 0.154$, and in Fig. 2b for $x = 0.290$. Below a temperature of 200 K, the thermoelectric power of the $CoZr_2$ crystal varies from sample to sample, both in the basal plane and along the $\langle 001 \rangle$ axis. Although the reproducibility of the thermoelectric power data for any particular sample was within the experimental accuracy, the differences between data for different samples with the same crystallographic orientation were much larger. These differences disappear at temperatures higher than 200 K. Figure 1 shows the results for two samples oriented along the $\langle 100 \rangle$ axis and along the $\langle 001 \rangle$ axis. Such behavior was also observed for samples with long dimensions in the $\langle 110 \rangle$ direction.

The probable cause of such large discrepancies between samples is an inhomogeneous distribution of structural defects in the crystals. The thermoelectric power at low temperatures is highly sensitive to defects and
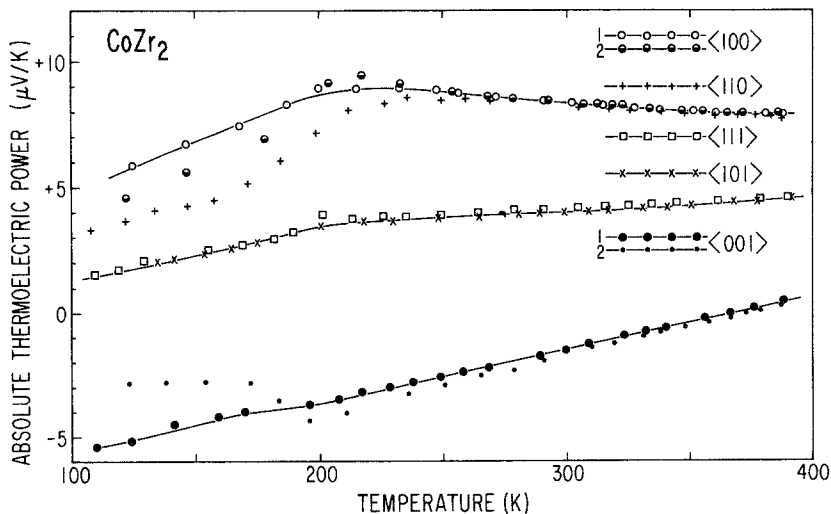

Fig. 1. Absolute thermoelectric power vs. temperature of $CoZr_2$ in different crystallographic directions. The data denoted by the numbers 1 and 2 refer to different samples along the same direction.
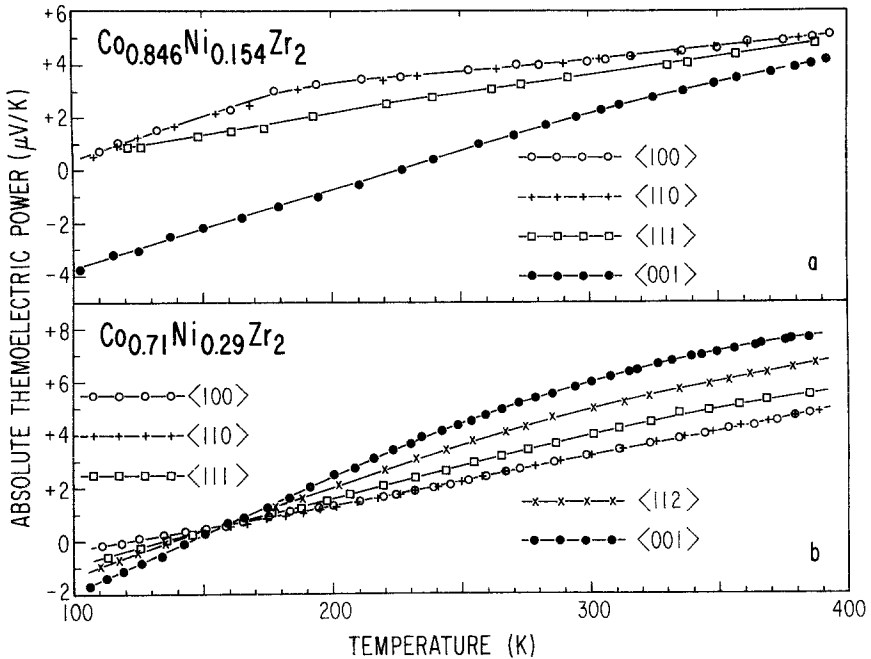
Fig. 2. Absolute thermoelectric power vs. temperature of (a) $Co_{0.846}Ni_{0.154}Zr_2$ and (b) $Co_{0.710}Ni_{0.290}Zr_2$.

impurity concentrations. It is therefore likely that those data for samples exhibiting the greatest thermoelectric power anisotropy for $CoZr_2$ are most representative of the true properties of this compound (see curves labeled 1 in Fig. 1).

No variation in the thermoelectric power of different samples with the same crystallographic orientation was observed for the crystals of $Co_{1-x}Ni_xZr_2$ with $x = 0.154$ and 0.290. It should be noted, however, that these crystals exhibited a smaller anisotropy. The large value of $\Delta T_c/\Delta x$ near $x = 0.290$ can be used to estimate the compositional gradients inside these samples. In a distance of about 1 cm, T_c of our single-crystal ingot was found to change by 0.2 K. The results of Havinga *et al.*[1] for the dependence of T_c on x show that such a value corresponds to a change in x of about 0.02. The large thermoelectric power anisotropy of the $Co_{1-x}Ni_xZr_2$ system varies slowly enough with composition that the final interpretation of the results presented here should be valid in spite of the slight compositional variation between samples prepared from the same crystal.

The large anisotropy of the normal state thermoelectric power prompted us to investigate other physical properties of the $Co_{1-x}Ni_xZr_2$

TABLE I

Magnetic Susceptibility χ at 294 K with the Applied Magnetic Field Parallel to the a and c Axes $\chi_{\|a}$ and $\chi_{\|c}$ and the Ratio $\chi_{\|a}/\chi_{\|c}$ for $Co_{1-x}Ni_xZr_2$ for $x = 0$, 0.154, and 0.29[a]

x	$\chi_{\|a}$, 10^{-6} cm^3/g	$\chi_{\|c}$, 10^{-6} cm^3/g	$\chi_{\|a}/\chi_{\|c}$	$\bar{\chi}$, 10^{-6} cm^3/g
0	2.114	2.049	1.032	2.092
0.154	2.173	2.042	1.064	2.129
0.29	2.129	1.955	1.089	2.071

[a]The reproducibility and absolute accuracy of the χ values are estimated to be 0.1% and 1%, respectively. Also shown are derived values for the average susceptibility $\bar{\chi}$, where $\bar{\chi} \equiv (\chi_{\|c} + 2\chi_{\|a})/3$.
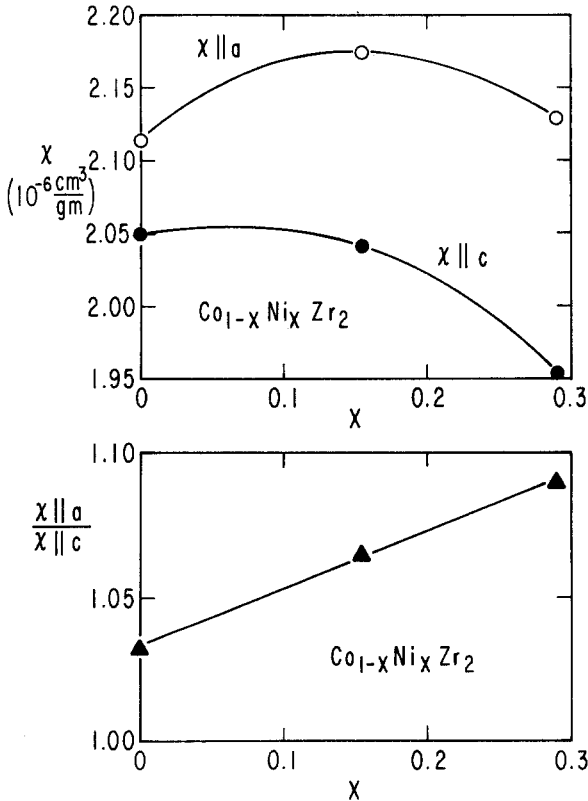

Fig. 3. Mass magnetic susceptibility χ at 294 K with the applied magnetic field parallel to the a and c axes, $\chi_{\|a}$ and $\chi_{\|c}$, and the ratio $\chi_{\|a}/\chi_{\|c}$, vs. x for $Co_{1-x}Ni_xZr_2$.

system with respect to the question of anisotropic behavior. First, the static magnetic susceptibility of single-crystal specimens of Co$_{1-x}$Ni$_x$Zr$_2$ with $x = 0$, 0.154, and 0.290 was measured with the applied magnetic field aligned along the $\langle 100 \rangle$ axis ($\chi_{\|a}$) and along the $\langle 001 \rangle$ axis ($\chi_{\|c}$) by means of the Faraday method at 294 K. The values obtained for $\chi_{\|a}$ and $\chi_{\|c}$, as well as the ratio $\chi_{\|a}/\chi_{\|c}$, are given in Table I, while plots of these quantities vs. x are shown in Fig. 3. The ratio $\chi_{\|a}/\chi_{\|c}$ is greater than unity and increases linearly with x for the three samples that were investigated. However, both $\chi_{\|a}$ and $\bar{\chi} \equiv (\chi_{\|c} + 2\chi_{\|a})/3$ (cf. Table I) exhibit maxima for $x = 0.154$. Thus, these two quantities both correlate with the occurrence of the T_c maximum near $x = 0.15$ in the Co$_{1-x}$Ni$_x$Zr$_2$ system, as cited in Section 1. Second, the electrical resistivity ρ as a function of temperature between 2 and 290 K of single-crystal specimens of Co$_{1-x}$Ni$_x$Zr$_2$ with $x = 0$ and 0.21 was measured using an ac four-probe technique with the current flowing along

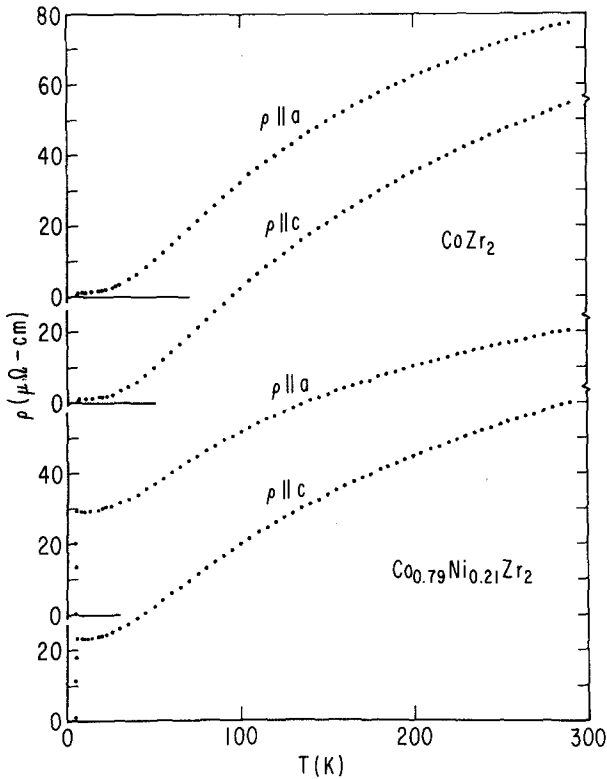Fig. 4. Electrical resistivity parallel to the a and c axes, $\rho_{\|a}$ and $\rho_{\|c}$, vs. temperature T for CoZr$_2$ and Co$_{0.790}$Ni$_{0.210}$Zr$_2$.
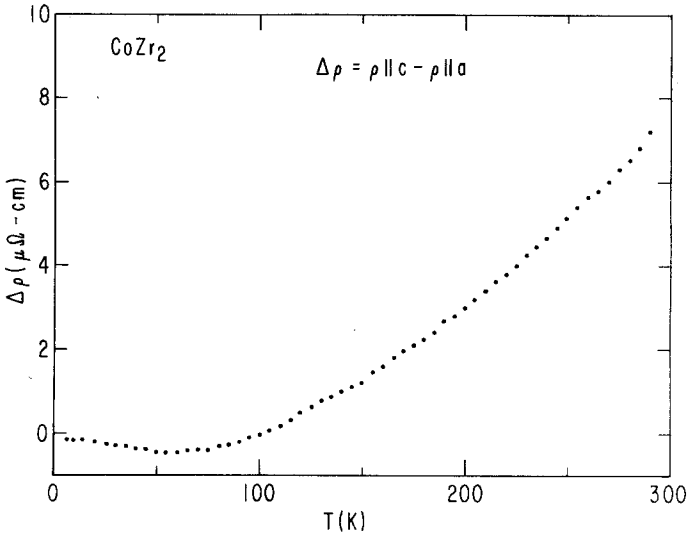
Fig. 5. Difference $\Delta\rho(T) \equiv \rho(T)_{\|c} - \rho(T)_{\|a}$ vs. temperature T for CoZr$_2$.

the $\langle 100 \rangle$ axis ($\rho_{\|a}$) as well as along the $\langle 001 \rangle$ axis ($\rho_{\|c}$). Plots of $\rho_{\|a}$ and $\rho_{\|c}$ vs. temperature for CoZr$_2$ and Co$_{0.79}$Ni$_{0.21}$Zr$_2$ are displayed in Fig. 4. From the figure, it can be seen that the temperature-dependent contribution to the electrical resistivity $\rho(T)$ above 4 K increases more rapidly with temperature for $\rho_{\|c}$ than for $\rho_{\|a}$ for both values of x. This is illustrated in Figs.
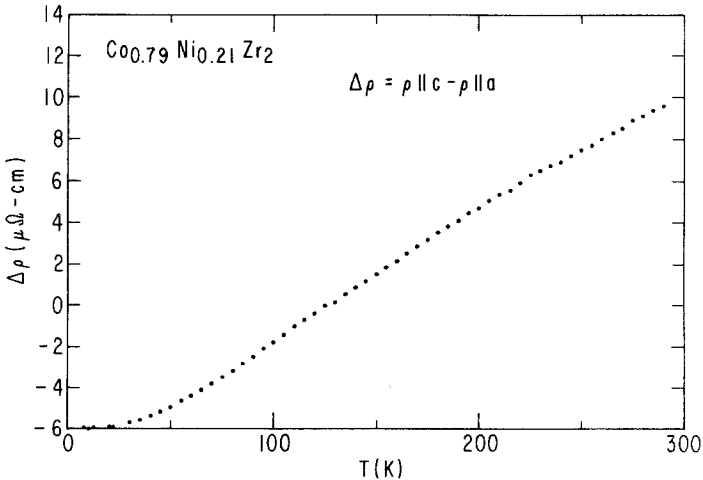

Fig. 6. Difference $\Delta\rho(T) \equiv \rho(T)_{\|c} - \rho(T)_{\|a}$ vs. temperature T for Co$_{0.790}$Ni$_{0.210}$Zr$_2$.

5 and 6, where the difference $\Delta\rho(T) \equiv \rho(T)_{\|c} - \rho(T)_{\|a}$ is plotted vs. temperature for $CoZr_2$ and $Co_{0.79}Ni_{0.21}Zr_2$, respectively.

4. DISCUSSION

Regardless of crystallographic orientation, the thermoelectric power of each of the $Co_{1-x}Ni_xZr_2$ crystals decreased from its positive value at room temperature as the sample cooled and, in some cases, actually became negative. This result implies that the thermoelectric power has a negative hump at least below $0.4\theta_D$, where the Debye temperature θ_D lies between 240 and 250 K for the compositional range examined.[5]

Phonon drag effects can produce positive thermoelectric power peaks in isotropic metals at temperatures in the range $(0.1-0.2)\theta_D$ and negative ones in anisotropic metals.[10] Highly anisotropic at low temperatures, the polyvalent metals Mg, Co, and Zn show positive or negative thermoelectric power maxima attributable to the phonon drag contribution due to small portions of the Fermi surface.[11] However, it has also been found that second-order, intrinsic two-phonon processes[12] or higher order electron–phonon processes[13] may give a significant contribution to the electron diffusion thermoelectric power at low temperatures. They can cause the thermoelectric power to exhibit a negative peak in the range $(0.3-0.5)\theta_D$ and to decrease as $1/T$ as the temperature T increases above θ_D.[13]

Figure 7 shows $S_\perp(T)$, the thermoelectric power measured parallel to the $\langle 100 \rangle$ axis. For $x = 0$, $S_\perp(T)$ is positive and shows a pronounced positive
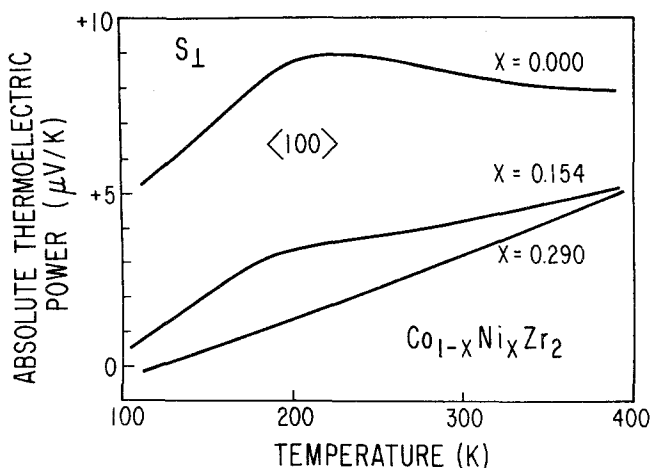

Fig. 7. Temperature dependence of the thermoelectric power of $Co_{1-x}Ni_xZr_2$ parallel to the a axis for $x = 0$, 0.154, and 0.290.

hump near $T = \theta_D$. As x increases to 0.154., both the value of $S_\perp(T)$ and the amplitude of the hump decrease. For $x = 0.290$, $S_\perp(T)$ is almost a linear function of temperature. Displayed in Fig. 8 is a graph of $S_\perp/T$ vs. $1/T^2$ for $T > 250$ K and $x = 0$. The open and half-shaded circles represent the data for two different samples. A linear least squares fit to the data yields the following expression for the thermoelectric power as a function of temperature for $T > 250$ K and $x = 0$ in units of $\mu V/K$:

$$S_\perp(T) = 9.855 \times 10^{-3} T + 1607 T^{-1} \tag{1}$$

This particular functional form can be viewed in terms of two contributions to the diffusion thermopower: (1) a normal one S_n^e proportional to T, and (2) a low-temperature one S_l^e proportional to $1/T$. It is quite surprising that at 300 K, $S_l^e = +5.36 \, \mu V/K$ and $S_n^e = +2.96 \, \mu V/K$, so the low-temperature contribution is nearly twice as large as the normal component.

Theory[14] has shown that the diffusion thermoelectric power S^e is generally determined by the energy dependence of the electrical conductivity. An approximate expression for S^e is

$$S^e = -\frac{(\pi k_B)^2}{3|e|} T\left[\frac{d \ln L(E)}{dE} \times \frac{d \ln A(E)}{dE}\right]_{E=E_F} \tag{2}$$

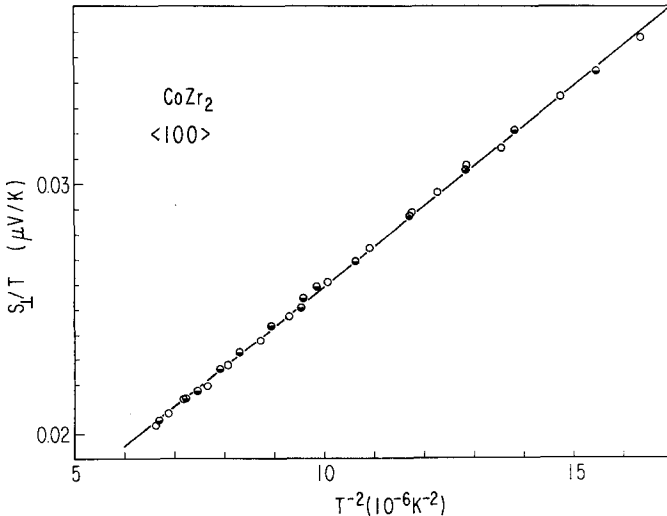The first and second terms represent the energy dependence of the mean

Fig. 8. The thermoelectric power S of CoZr$_2$ for temperatures $T > 250$ K plotted as ST^{-1} vs. T^{-2}. The straight line was fitted to the data by the method of least squares.

free path L near the Fermi energy E_F and of the Fermi surface area A, respectively. Here e is the electronic charge and k_B is the Boltzmann constant. A hole-like surface gives a decreasing number of states with increasing Fermi energy and contributes to the thermoelectric power with a sign opposite to that of an electron-like one.

In the Co$_{1-x}$Ni$_x$Zr$_2$ system, $L(E)$ cannot be associated with a single scattering mechanism, and modification of the band structure probably occurs with increasing x. Because it is a d-band system, a large contribution to the electrical resistivity is expected due to scattering of s electrons into the high-density-of-states d band. Mott's model of isotropic s–d scattering[15] predicts that L is inversely proportional to the density of states $N(E)$. Hence, there is a contribution S_d^e to S^e given by

$$S_d^e = +\frac{(\pi k_B)^2}{3|e|}\, T \left[\frac{d \ln N(E)}{dE}\right]_{E=E_F} \qquad (3)$$

as well as terms due to solute atom resistivity and deviations from Matthiessen's rule. Evidence for s–d scattering is provided by the negative curvature of the ρ vs. T data displayed in Fig. 4.

A shift of the Fermi level across the d band due to alloying is expected to strongly influence the diffusion thermoelectric power, particularly when the Fermi level is near the upper or lower band edges. Such an effect has apparently been observed for Ag$_{1-x}$Pd$_x$.[16] In this system there is a sudden decrease in the thermoelectric power at a rate $\Delta S/\Delta x = -200 \,\mu$V/K to a large negative value near $x = 0.5$. Similar thermoelectric power behavior has been observed for Fe$_{1-x}$Ni$_x$Al.[17] In such cases the S_d^e term can be assumed to be dominant.

The average thermoelectric power $\bar{S}$ of the Co$_{1-x}$Ni$_x$Zr$_2$ system is given in Table II, with the definition $\bar{S} \equiv (S_\| + 2S_\perp)/3$. It changes by a mere

TABLE II

Thermoelectric Power S Parallel to a and c Axes $S_\perp$ and $S_\|$, Average $\bar{S}$, and $dT/dS_{\perp,\|}$ for Co$_{1-x}$Ni$_x$Zr$_2$ for $x = 0, 0.154, 0.29$[a]

T, K	x	$S_\perp$, μV/K	$S_\|$, μV/K	$\bar{S}$,[b] μV/K	$dT/dS_\perp$, K$^2/\mu$V	$dT/dS_\|$, K$^2/\mu$V	
250	0	8.80	-2.57	5.01	-94.3	45.1	2.27
	0.154	3.82	0.78	2.81	111	33	1.08
	0.290	2.23	4.38	2.91	51.7	27.9	-0.74
390	0	7.90	0.48	5.43	-476	45.1	1.37
	0.154	5.08	4.20	4.79	95	50	0.18
	0.290	4.95	7.80	5.90	51.7	124	-0.48

[a] Also shown is the anisotropy parameter $(S_\perp - S_\|)/\bar{S}$. $S_\perp$, $\langle 100 \rangle$ axis, $S_\|$, $\langle 001 \rangle$ axis.
[b] $\bar{S} = (S_\| + 2S_\perp)/3$.

$-2\,\mu\text{V/K}$ at 250 K and by only $\pm0.6\,\mu\text{V/K}$ at 390 K as x changes from 0 to 0.290. As shown in Table II, the dependence of $S_\perp$ or $S_\parallel$ on x is larger than that of $\bar{S}$ but still small enough to show that S_d^e is not a dominant term. This indicates that $N(E_F)$ does not change appreciably as x varies from 0 to 0.290, consistent with the magnetic susceptibility data in Table I and Fig. 3.

Figure 9 presents the $S_\parallel(x, T)$ data for the $Co_{1-x}Ni_xZr_2$ system. Note that $S_\parallel(x, T)$ increases as either x or T increases. Above 200 K, $S_\parallel$ increases linearly with temperature for $x = 0$. When $x = 0.154$ or 0.290, $S_\parallel(T)$ deviates from linearity as $-A(x)T^{4.5}$, with the constant $A(x = 0.290)$ over three times larger than $A(x = 0.154)$.

As x is varied, both the value and the character of the temperature dependence of $S_\perp(T)$ change in the opposite respective fashion from those of $S_\parallel(T)$. There is a decrease in $S_\perp(T)$ as x increases, and its nonlinear temperature behavior above θ_D may be treated by adding to the linear dependence a term B/T, with the constant B decreasing with increasing x. At the same time there is an increase in $S_\parallel(T)$ as x increases, and its deviation from linearity may be described by including a term $-AT^{4.5}$, with the constant A increasing with increasing x. Such behavior of $S_\perp(x, T)$ and $S_\parallel(x, T)$ is responsible both for the smallest thermoelectric power anisotropy $(S_\perp - S_\parallel)/\bar{S}$ being associated with the composition $(x \approx 0.2)$ close to that possessing the highest T_c and for the opposite signs of the anisotropy
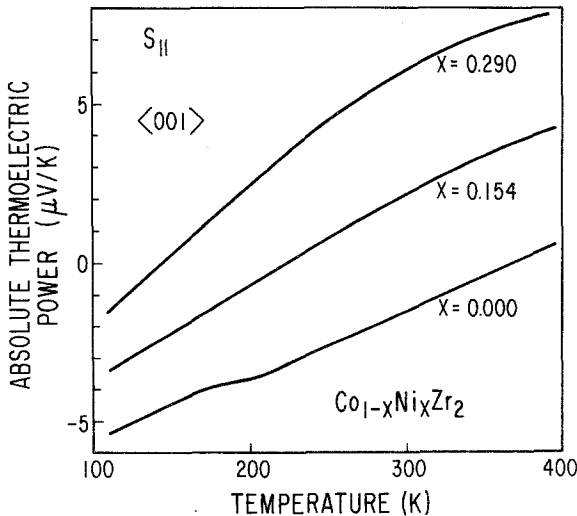

Fig. 9. The thermoelectric power of $Co_{1-x}Ni_xZr_2$ along the unique crystallographic axis vs. temperature for $x=0$, 0.154, and 0.290.

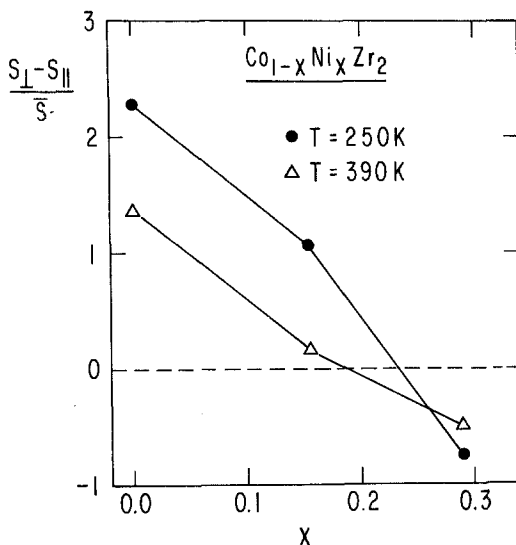Fig. 10. Thermoelectric power anisotropy parameter $(S_\perp - S_\parallel)\bar{S}$ vs. composition x for Co$_{1-x}$Ni$_x$Zr$_2$ at 250 K and 390 K.

as x increases or decreases from that composition (see Table II), as shown in Fig. 10.

The expected smearing out of the Fermi surface with alloying does not have a well-defined pronounced effect on the anisotropy of the thermoelectric power, and it is very probable that the anisotropy in phonon dynamics plays an important role in determining both $S(T)$ and its anisotropy in the Co$_{1-x}$Ni$_x$Zr$_2$ system.

It is possible that some particular contribution to the thermoelectric power could have been dominant for some crystal directions in the temperature and composition ranges examined here, so the complete thermoelectric power characterization of this system cannot be generalized at this stage.

For uniaxial systems the thermoelectric power in some arbitrary direction relative to the principal axis, often referred to as the isothermal power, is given by Thomson's rule:

$$S(\theta) = S_\perp \sin^2 \theta + S_\parallel \cos^2 \theta \qquad (4)$$

where θ is the angle between the arbitrary direction and the unique principal axis. Values of $S(\theta)$ calculated from the data in Table II utilizing Eq. (4) for Co$_{1-x}$Ni$_x$Zr$_2$ at 250 and 390 K are presented in Table III. It can be seen that there is practically no anisotropy in the basal plane. In the other

TABLE III

Measured and Calculated Thermoelectric Power S at 250 and 390 K Along the $\langle 110 \rangle$, $\langle 112 \rangle$, $\langle 111 \rangle$, and $\langle 101 \rangle$ Directions[a]

	$S(250\ \text{K})$, $\mu\text{V/K}$					
Axis	$x=0$		$x=0.154$		$x=0.290$	
	S_m	S_c	S_m	S_c	S_m	S_c
$\langle 110 \rangle$	8.60	8.80	3.82	3.82	2.23	2.23
$\langle 112 \rangle$	—	—	—	—	3.62	3.50
$\langle 111 \rangle$	3.90	5.69	2.98	3.01	2.85	2.80
$\langle 101 \rangle$	3.80	3.90	—	—	—	—

	$S(390\ \text{K})$, $\mu\text{V/K}$					
Axis	$x=0$		$x=0.154$		$x=0.290$	
	S_m	S_c	S_m	S_c	S_m	S_c
$\langle 110 \rangle$	7.80	7.90	5.08	5.08	4.95	4.95
$\langle 112 \rangle$	—	—	—	—	6.78	6.63
$\langle 111 \rangle$	4.60	5.87	4.88	4.84	5.60	5.70
$\langle 101 \rangle$	4.50	4.70	—	—	—	—

[a]The calculated values S_c were computed from the measured values S_m along the $\langle 100 \rangle$ and $\langle 001 \rangle$ principal axes as explained in the text.

directions Thomson's rule is satisfied, except for the $\langle 111 \rangle$ direction of $CoZr_2$. However, for this particular orientation only one sample was measured, and the result may be spurious.

The most characteristic feature of the $S(T)$ data for the $Co_{1-x}Ni_xZr_2$ system is its anisotropy, and data for dT/dS, $S_\perp$, and $S_\parallel$ at 250 and 390 K have been summarized in Table II.

The measurements reported here reveal anisotropic behavior of the normal state thermoelectric power, electrical resistivity, and magnetic susceptibility of the superconducting $Co_{1-x}Ni_xZr_2$ system. Further investigations would be useful in correlating the anisotropic behavior of the normal and superconducting state physical properties of $Co_{1-x}Ni_xZr_2$ compounds, and in establishing the features in the interacting electron and phonon systems that are responsible for the interesting superconducting properties of $Co_{1-x}Ni_xZr_2$ and other compounds with the C-16 crystal structure.

REFERENCES

1. E. E. Havinga, H. Damsma, and J. M. Kanis, *J. Less-Common Metals* **27**, 281 (1972).

2. K. Tagano, K. Kyoji, and K. Tachikawa, *J. Less-Common Metals* **33**, 275 (1973).
3. K. Tagano and K. Tachikawa, *Phys. Lett.* **54A**, 205 (1975).
4. F. R. Eshelman and J. F. Smith, *J. Appl. Phys.* **46**, 5080 (1975).
5. E. E. Havinga and M. H. van Maaren, *Phys. Rep. Phys. Lett. C* **10C**, 107 (1974).
6. B. T. Matthias, in *Progress in Low Temperature Physics*, Vol. II, C. J. Gorter, ed. (North-Holland, Amsterdam, 1957), p. 138.
7. K. Yamaha, T. Sambongi, and T. Mitsui, *J. Phys. Soc. Japan* **26**, 866 (1969).
8. S. L. McCarthy, *J. Low Temp. Phys.* **4**, 489 (1971).
9. N. Cusack and P. Kendall, *Proc. Phys. Soc.* **72**, 898 (1958).
10. J. M. Ziman, *Phil. Mag.* **4**, 371 (1959).
11. V. A. Rowe and P. A. Schroeder, *J. Phys. Chem. Solids* **31**, 1 (1970).
12. P. E. Nielson and P. L. Taylor, *Phys. Rev. B* **10**, 4061 (1974).
13. A. Hasegawa, *J. Phys. F: Metal Phys.* **4**, 2164 (1974).
14. J. M. Ziman, *Electrons and Phonons* (Clarendon Press, Oxford, 1972), p. 397.
15. N. F. Mott, *Proc. Roy. Soc. A* **156**, 368 (1936); *Adv. Phys.* **13**, 325 (1964).
16. J. C. Taylor and B. R. Coles, *Phys. Rev.* **102**, 27 (1956).
17. F. A. Sidorenko, A. P. Kotov, L. P. Zelenin, B. M. Bronfin, and P. B. Gel'd, *Fiz. Metal Metalloved.* **34**, 1056 (1972).